Intelligent Energy Coordination and Harmonic Reduction for Islanded Microgrids Using ANFIS

Devireddy Sathish[1], Pannala Krishna Murthy[2], Narri Yadaiah[3]

[1,3]*Department of Electrical and Electronics Engineering, Jawaharlal Nehru Technological University, Hyderabad, India*

[2]*Department of Electrical and Electronics Engineering, Jayaprakash Narayan College of Engineering, Mahbubnagar, India.*

***Abstract*—This paper presents an ANFIS based energy management framework for an islanded microgrid, integrating photovoltaic generation, wind energy conversion, and battery storage to coordinate the operation of multiple distributed energy sources. The existing methodology utilizes a Fuzzy Logic Controller (FLC) require expert knowledge for designing rules and membership functions, making tuning difficult. Hence, it endures from rule explosion and computational complexity as the number of input increases. To address the limitations of fixed membership functions and predefined fuzzy rules, ANFIS is trained using input output data obtained from the FLC. During training, the membership function parameters are iteratively updated to minimize the deviation between the ANFIS and FLC outputs. The developed strategy aims to enhance control adaptability under varying renewable energy conditions and reduce harmonic distortion in the islanded microgrid. After training, the optimized membership functions and fuzzy rules enable ANFIS to generate an approximated control output for the given input variables. Simulation results demonstrate improved dynamic response, enhanced active power transfer, superior energy management, and lower harmonic distortion compared with the FLC based control approach.**

***Index Terms*—ANFIS, PV array, Wind turbine, Battery.**

I. INTRODUCTION

As the penetration of renewable generation continues to increase in modern power systems, effective control techniques are essential to ensure stable, and efficient operation of hybrid systems. Among the emerging solutions, islanded microgrids provide an independent electrical network capable of supplying power to consumers without relying on the main grid [1, 2]. The adoption of non-conventional sources can reduce dependence on conventional fossil fuel based generation and promote environmentally sustainable electricity production. IMS are especially suitable for remote and rural areas where connection to main grid involve considerable technical challenges and infrastructure costs [3,4]. By producing and managing electrical power near the consumer, such systems can improve energy availability and provide a flexible and economical means of supplying electricity to geographically isolated communities [5,6].

The integrated renewable energy sources consisting of PV and wind generation units along with a Battery, which are coordinated and connected to point of common coupling (PCC) as depicted in Fig.1 [7,8]. The solar PV system is connected to the PCC via DC-DC converter and 3-phase voltage source inverter (VSI) [9,10]. The wind turbine is connected to PCC via rectifier and inverter [12,13]. The Battery is connected to a PCC via bidirectional converter and inverter [14,15].

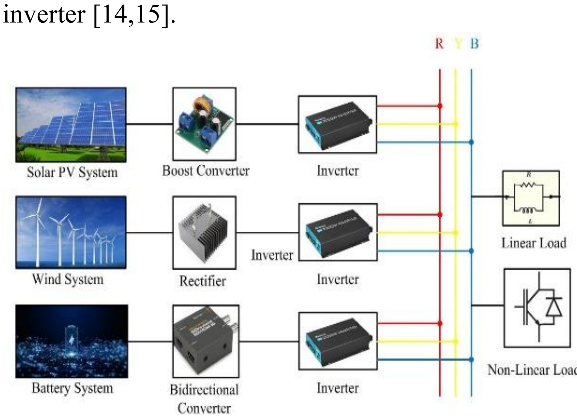

Fig. 1. Overall representation of islanded microgrid system.

The energy management system regulates the distribution of generated and stored energy by coordinating the PV array, wind turbine, and BESS according to the instantaneous load demand, thereby supporting a balanced power flow within the IMS [15], [16]. When renewable sources generate more than the load demand, the surplus power is stored in the BESS by operating the battery in charging mode. If renewable generation falls below the load demand, the battery changes to discharging mode and releases the stored energy to compensate for the deficit and sustain the required power supply.

Droop-based control is widely adopted in islanded microgrids because it enables distributed generation units to share load power without relying on a centralized communication link. By modifying the operating frequency and voltage magnitude in response to variations in active and reactive power, the droop mechanism facilitates decentralized power sharing among the distributed sources [17]. However, conventional droop control can introduce deviations in voltage and frequency and may result in inaccurate reactive power distribution, particularly when the feeder impedances of the connected units are unequal [18]. To address these limitations, virtual impedance techniques, including virtual resistance and virtual conductance, have been incorporated into microgrid control schemes to enhance system stability and improve power-quality characteristics [19], [20]. In addition, fuzzy logic controller (FLC)-based techniques provide improved adaptability under changing generation and loading conditions by incorporating nonlinear control rules, offering an alternative to conventional proportional-integral (PI) control methods [21], [22].

The remaining manuscript is presented as follows, Section 2 presents FLC based control structure in the islanded microgrid, Section 3 illustrates the ANFIS implementation for the islanded microgrid system and discusses the coordinated energy management strategy for the hybrid renewable energy sources, Section 4 provides the simulation results and a comparative assessment of the FLC and ANFIS. Finally, Section 5 finalizes the conclusion and future scope.

II. EXISTING CONTROL APPROACHES

In Photo voltaic subsystem, the boost converter is operated using a maximum power point tracking technique i.e. A perturb and observe (P&O) to maximize utilization of available power while maintaining the required DC link voltage, as depicted in Fig. 2 [11]. The fuzzy logic controller receives two input variables such as DC link voltage Vdc and change in power ΔP, with these inputs , it produces the required control signals, which are supplied to the PWM generator. The PWM pulses regulate the inverter switching operation to achieve the desired voltage and frequency at the PCC [23]. This coordinated control improves power quality during variations in operating conditions.

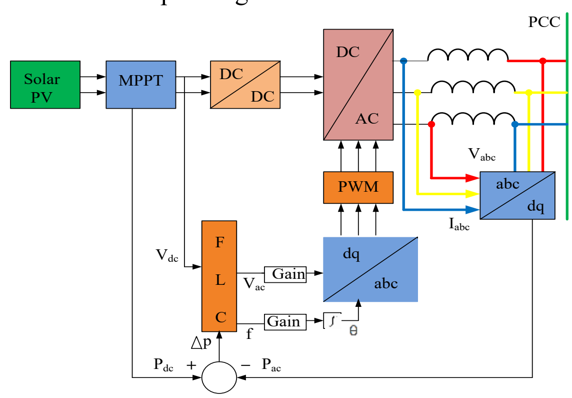

Fig.2 Schematic representation of voltage and frequency regulation

The wind energy conversion system comprises of DC-DC converter, permanent magnet synchronous generator, and 3-phase inverter as depicted in Fig.3. Maximum power extraction from the wind turbine is obtained by the P & O based tracking algorithm. The controller process the measured PV voltage and current to generate suitable gate pulses for the boost converter , there by controlling the power transfer and maintaining the DC-link voltage at the desired level [24, 25].

The input variables to the FLC are the DC link voltage V_{dc} and the change in the active power ΔP and it is used to generate the control signal based on the input values using a power angle control strategy. The control signal is then fed to the PWM generator that generates the desired switching pulses to the inverter. The inverter produces the voltage and frequency at PCC [23].

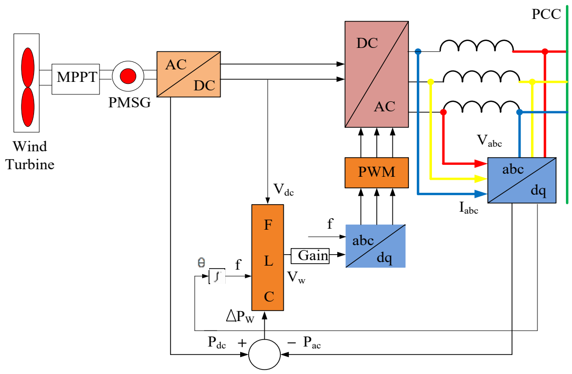

Fig.3 Schematic representation of power angle control scheme

Fuzzy control techniques are suitable for renewable energy application because they can handle complex nonlinear behaviour without depending on a precise system model. Nevertheless, the effectiveness of an FLC is influenced by the design of its membership functions and rule structure. To address this challenge, an ANFIS is introduced to refine its parameters through training data. This approach enhances the controllers ability to respond to changing operating conditions and improves the dynamic behaviour of the IMS .

III. DEVELOPMENT OF AN ADAPTIVE NEURO FUZZY CONTROL STRATEGY FOR ISLANDED MICROGRIDS

An ANFIS controller is developed for the IMS to achieve efficient energy management and improved power quality in the islanded microgrid system. The ANFIS combines the neural network based learning with fuzzy inference to improve the nonlinear system behaviour. It uses the training the data, enabling tuning of membership functions and inference parameters [26,27].

The FLC generates input-output data which are fed to the ANFIS to train the system by backpropagation learning algorithm. The developed controller generates the control signal required for inverter operation. A PWM modulator processes this signal to produce the corresponding gate pulses, which are applied to the inverter switching devices. The resulting switching action controls the inverter output, enabling the required AC voltage magnitude and operating frequency to be maintained at the PCC as shown in Fig.4

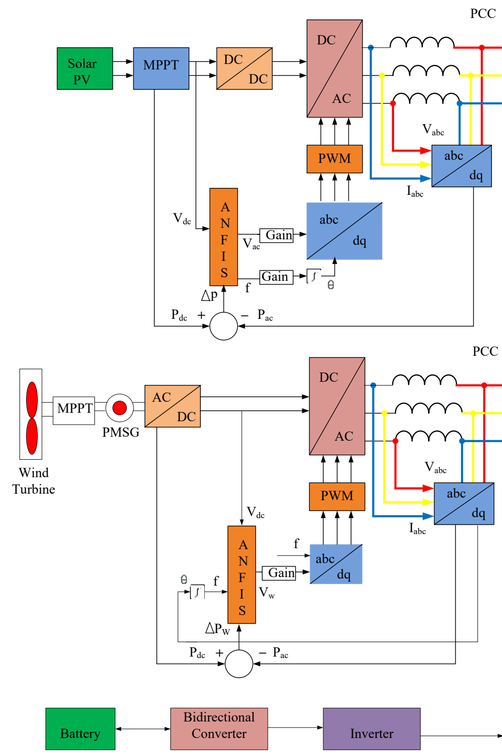

Fig. 4. Integrated control block diagram of the islanded microgrid system.

3.1 Framework of the ANFIS Controller

The developed ANFIS controller consists of five layers of computation - two adaptive layers and three fixed layers and it has two input variables V_{dc}, ΔP. The first layer defines the membership functions which perform the translation of the variables used in the input to their respective membership grade. These grades are then processed in the second layer where the fuzzy rules are created by fuzzifying the two inputs together. In the third layer, the activation levels of the individual rules are scaled according to their combined activation, normalized rule strengths for subsequent processing. The fourth layer to determine the next part of each rule using the adjustable consequent parameters. The consequent parameters are estimated during the forward-learning phase using the normalized firing strengths and the training input-output data. For the first-order Sugeno model, these parameters form the linear coefficients of the rule consequent functions and are determined through least-squares estimation. During the subsequent backward-learning phase, the premise parameters are updated using gradient descent based on the output error. Finally, as seen in Fig. 5, the fifth layer combines the output from all of the fuzzy rules to produce the overall ANFIS controller output.

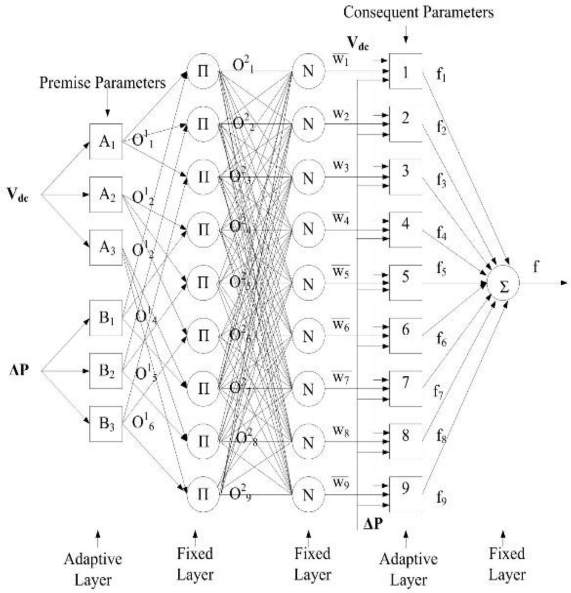

Fig.5 Framework of ANFIS controller

Layer 1: Adaptive Layer: Input Membership Functions

Layer 1 receives the two input crisp inputs: V_{dc}, Δ P.Each input has 3 membership functions: A_1, A_2, A_3, for V_{dc} and B_1, B_2, B_3 for ΔP . Therefore, Layer 1 has 6 adaptive nodes and this layer is called adaptive because its premise parameters are adjustable during training.

$O_i^1 = \mu\, A_i(V_{dc})$, i = 1,2,3

$O_{i+1}^1 = \mu\, B_i\,(\Delta\, P)$ i = 1,2,3

Where A_i, B_i denote fuzzy sets, μ is a membership function.

Layer 2: Fixed Layer: Rule Firing Strength

In the rule layer, individual nodes correspond to the defined fuzzy rules. For each rule, its activation level is obtained by combining the membership values of the associated inputs, thereby implementing the fuzzy conjunction operation.

$O_i^2 = \qquad w_i = \mu\, A_i(V_{dc}) \times \mu\, B_i\,(\Delta\, P)$

Layer 3: Fixed Layer: Normalization

The firing strength of every rule is converted into a normalized form.

$$\bar{w}_i = \frac{w_i}{\sum_{j=1}^{n} w_j}$$

Layer 4: Adaptive Layer: Consequent Functions

- This is the second adaptive layer. Layer 4 receives the normalized firing strengths from Layer 3. Each rule has a consequent function. For a first-order Sugeno ANFIS, p_i, q_i, r_i are consequent parameters and rule i is represented by:

$$f_i = p_i x + q_i y + r_i$$

The output becomes

$$O_i^{(4)} = \bar{w}_i f_i$$

Layer 5: Fixed Layer: Aggregation

Layer 5 receives the nine outputs from Layer 4:

$$\text{Output} = \sum_{i=1}^{n} \overline{w}_i\ f_i$$

$$= \sum_{i=1}^{n} O_i^{(4)}$$

Layer 4 produces the output of each ANFIS rule, and Layer 5 adds all these rule outputs to obtain the final ANFIS output.

3.2 ANFIS Algorithm

Step 1: Specify the initial parameter values for ANFIS training

Set the initial membership-function parameters (a, b, c), Set the initial rule consequent parameters p_i, q_i, and r_i, learning rate η, error goal E_{goal}, maximum number of training epochs.

Step 2: Apply the training inputs

For each training sample k, apply:$V_{dc}(k)$, $\Delta P(k)$.

Step 3: Perform the forward pass

Membership grades→ Rule firing strengths→ Normalized firing strengths→ Consequent outputs→ Final output.

$y(k) = \sum_{i=1}^{9} \overline{w}_i\, f_i(k)$.

Step 4: Estimate consequent parameters using Lease square estimation method

The consequent parameters are estimated by minimizing:

$E = \sum_i^N [y_d(k) - y(k)]^2$

Step 5: Calculate the training error

After obtaining the ANFIS output, calculate the training error :

$E\,(k) = y_d(k) - y(k)$

Mean square error $= \frac{1}{N} \sum_{k=1}^{N} e^2(k)$

Case1: Error is within the limit

MSE $\leq$ E goal
The training process is stopped, and the trained ANFIS parameters are obtained.
Case 2: Error is greater than the limit
MSE > E goal
The hybrid learning algorithm continues to the backward pass. The algorithm does not directly modify the rule firing strengths. Instead, it updates the trainable parameters of the ANFIS network.
Step 6: Backpropagation for premise-parameter updating
The error is propagated backward from Layer 5 toward Layer 1.For each premise parameter θ, the gradient is calculated as:

$$\frac{\partial E}{\partial \theta}$$

The premise parameters are iteratively adjusted using a gradient-based learning mechanism to minimize the training error.

$$\theta_{new} = \theta_{old} - \eta \frac{\partial E}{\partial \theta}$$

For triangular membership functions, the parameters are:

$$\theta \in \{a, b, c\}$$

Therefore:

$$a_{new} = a_{old} - \eta \frac{\partial E}{\partial a}$$

$$b_{new} = b_{old} - \eta \frac{\partial E}{\partial b}$$

$$c_{new} = c_{old} - \eta \frac{\partial E}{\partial c}$$

These updates change the shape and position of the triangular membership functions.
This process continues until:
MSE $\leq$ E goal

IV. SIMULATION RESULTS AND DISCUSSION

The typical parameters of the integrated PV, wind, and battery energy systems are derived to construct the islanded microgrid model. These parameters are used as the simulation inputs to evaluate the developed control strategy under different operating conditions.
Table.1.

PV Aarry		Wind Turbine		Battery	
Power	2.4 Kw	Power	2.4 Kw	Rating	9 Kwh
I rs	1000 W/m^2	Density	1.25 Kg/m^3	L_b	0.1 e-3
Q	1.602× 10^{-19} C	radius	1.31 m	C_p	12000 e^{-6}
θ	298 K	V_w	12 m/s	Lifecycle	> 10,000
I src	8.12 A	η_{gear}	1	Lifetime	5- 8 Years
N_s (series Strings)	12	P(Pole Pairs)	4	Q rated	30 Ah
N_p(Parallel Strings)	1	ω rated	2300 rpm	SOC	60%

The developed ANFIS based energy management and harmonic mitigation scheme is assessed through a MATLAB/Simulink simulation model. The system is configured according to the parameters specified in the corresponding Table.1, which are chosen to represent islanded microgrid operating conditions.

The PV array, wind turbine and battery is operated different operating conditions and the simulation time is 1.3 sec.

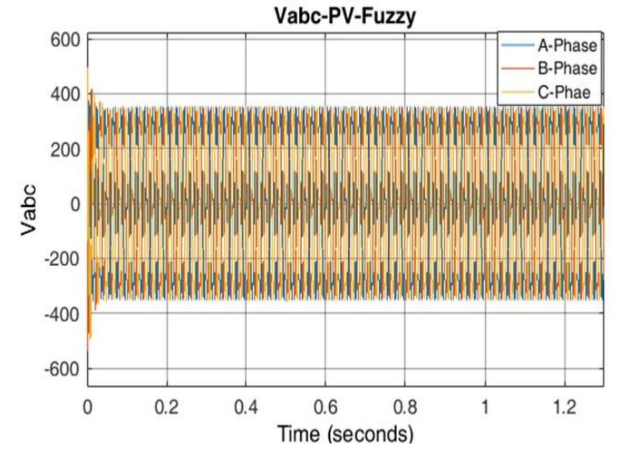

(a)

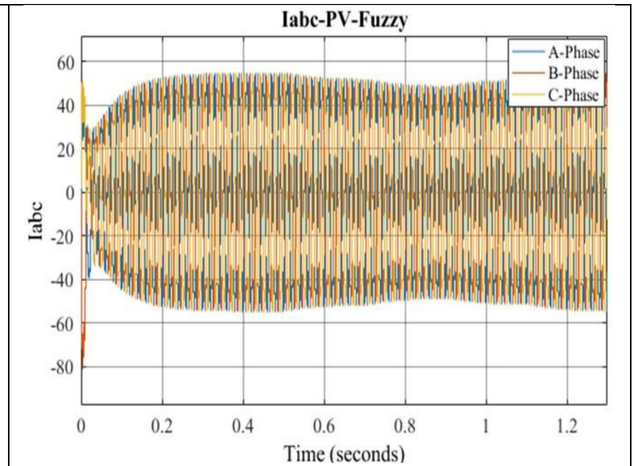

(b)

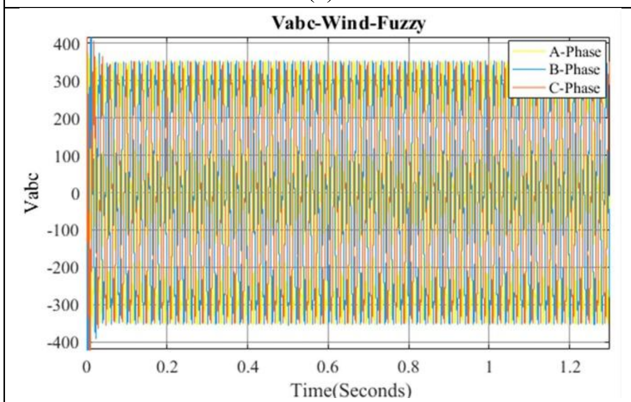

(c)

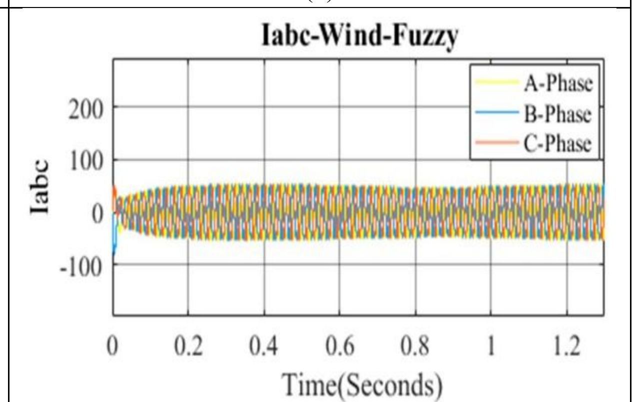

(d)

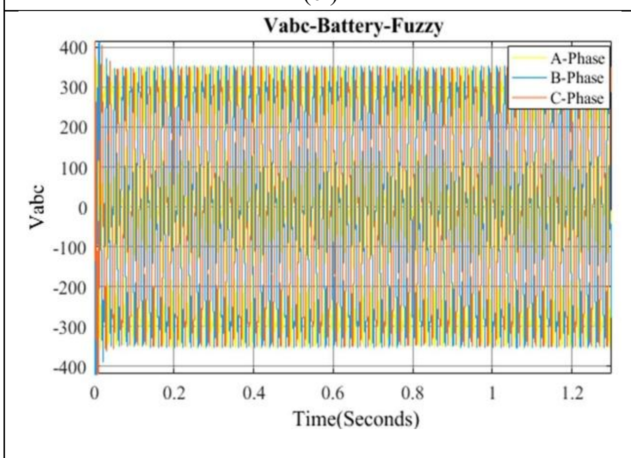

(e)

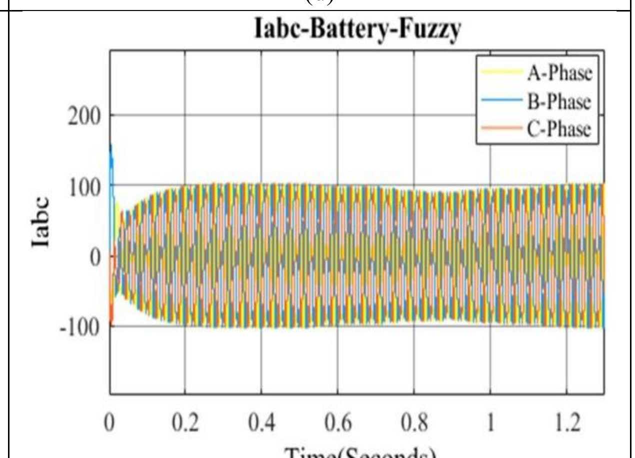

(f)

Fig.6 (a) PV array inverter output voltage, (b) PV array inverter output current, (c) Wind turbine inverter output voltage, (d) Wind turbine inverter output current, (e) Battery inverter output voltage, (f) Battery inverter output current.

The inverter output 3-phase voltage and current waveforms of the PV, wind, and battery units are presented in Fig. 6 (a), Fig 6 (b), Fig 6 (c), Fig 6 (d), Fig6 (e), Fig 6 (f) under fuzzy logic controller .The results exhibit a sinusoidal nature, while the corresponding THD values remain within the permissible limits specified by IEEE standards.

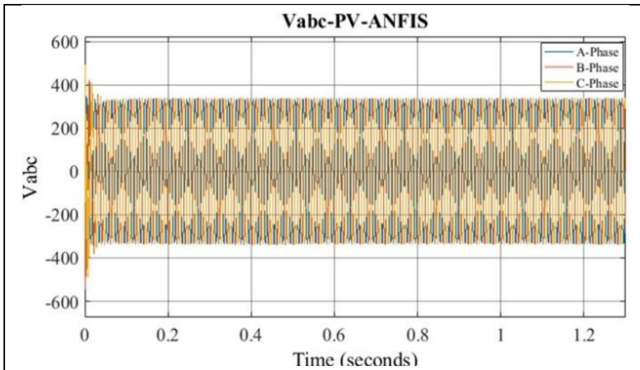

(a)

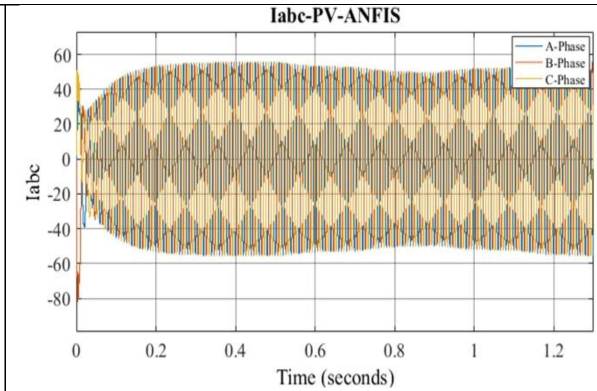

(b)

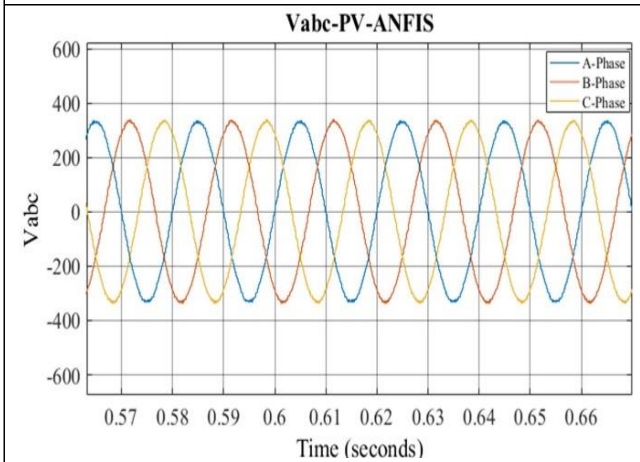

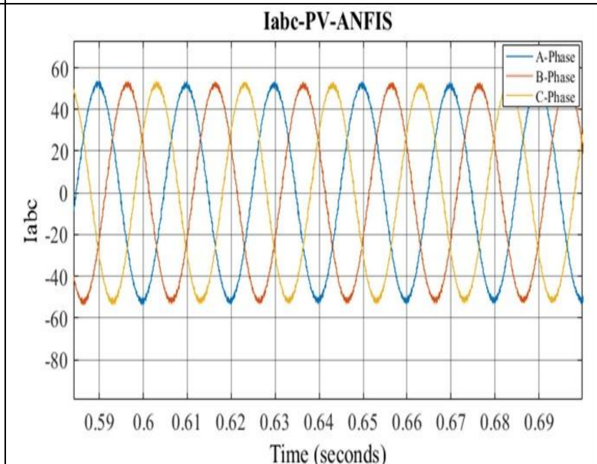

(c) (d)

Fig. 7. (a) PV inverter output voltage, (b) PV inverter output current, (c) PV inverter enlarged view of the output voltage, and (d) PV inverter enlarged view of the output current.

The PV inverter 3-phase voltage and current responses obtained with the ANFIS controller, along with their magnified waveforms, are shown in Fig. 7 (a), Fig 7 (b), Fig 7 (c) and Fig 7 (d). The results indicate that the inverter produces sinusoidal 3-phase voltage and current waveforms with reduced harmonic distortion compared with the fuzzy logic controller.

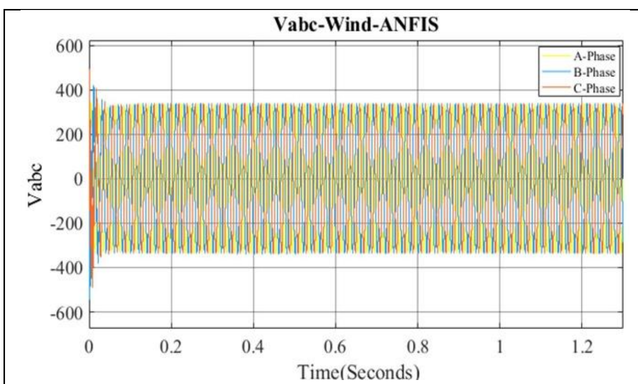

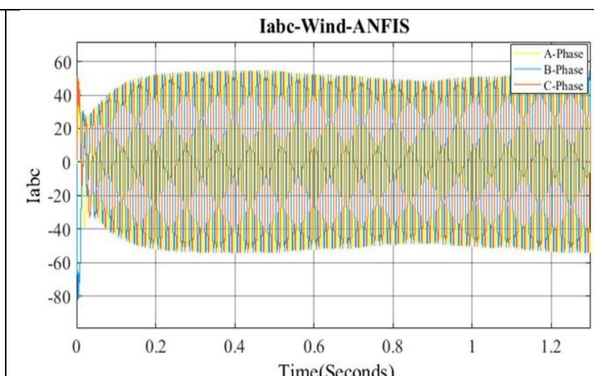

(a) (b)

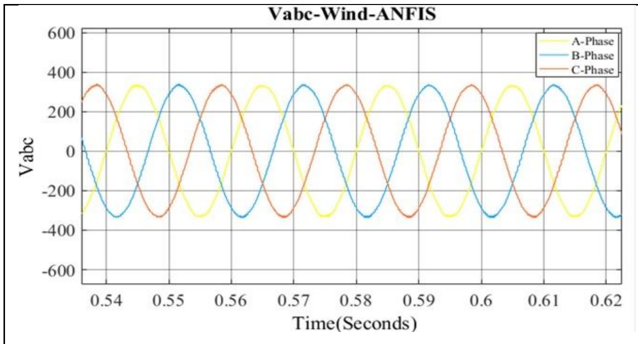

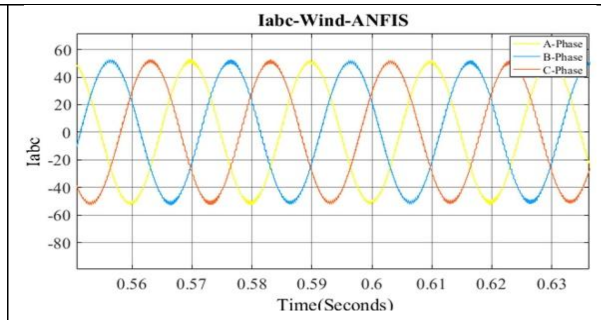

(c)	(d)

Fig. 8. a) Wind turbine inverter output voltage, (b) Wind turbine inverter output current, (c) Wind turbine magnified view of the output voltage, and (d) Wind turbine magnified view of the output current.

The three-phase voltage and current waveforms of the wind turbine inverter, together with their corresponding enlarged views, are presented in Fig. 8 (a), Fig 8 (b), Fig 8 (c) and Fig 8 (d) for the adaptive neuro fuzzy inference system control strategy. The obtained responses exhibit a sinusoidal waveform with reduced distortion, demonstrating improved inverter performance compared with the fuzzy logic controller.

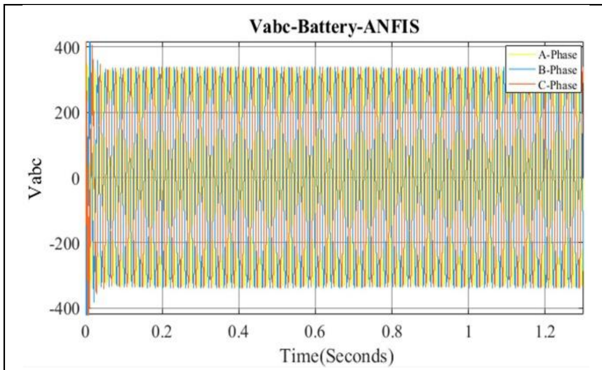

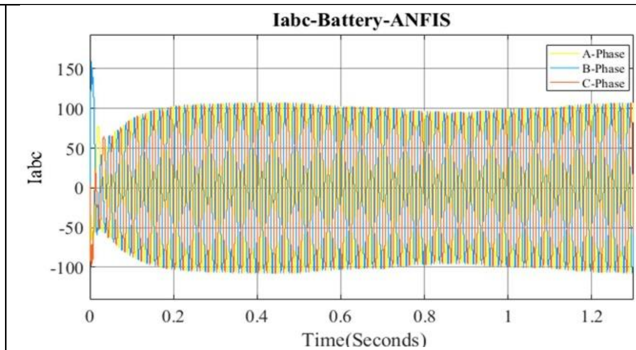

(a)	(b)

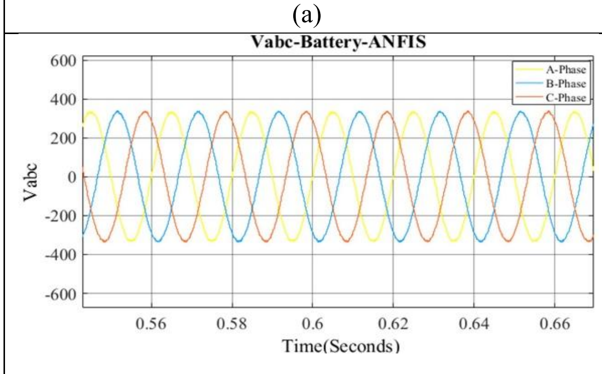

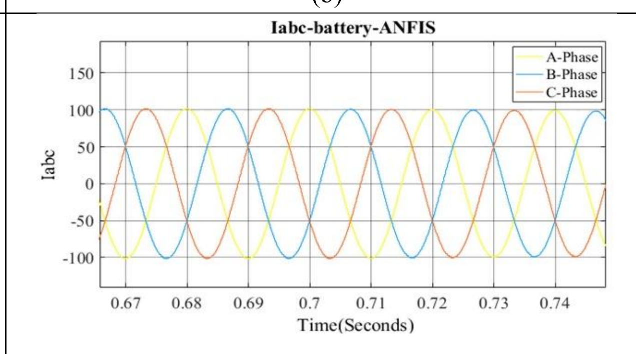

(c)	(d)

Fig. 9. Inverter-side electrical characteristics of the battery energy storage unit: (a) voltage waveform, (b) current waveform, (c) enlarged voltage waveform, and (d) enlarged current waveform.

The inverter side voltage and current waveforms of the battery system are illustrated in Fig. 9 (a) and 9 (b), while their enlarged views are shown in Fig. 9 (c) and 9 (d). The results indicate that the ANFIS based control scheme produces smooth and sinusoidal voltage and current waveforms at the battery inverter output compared to the fuzzy logic controller.

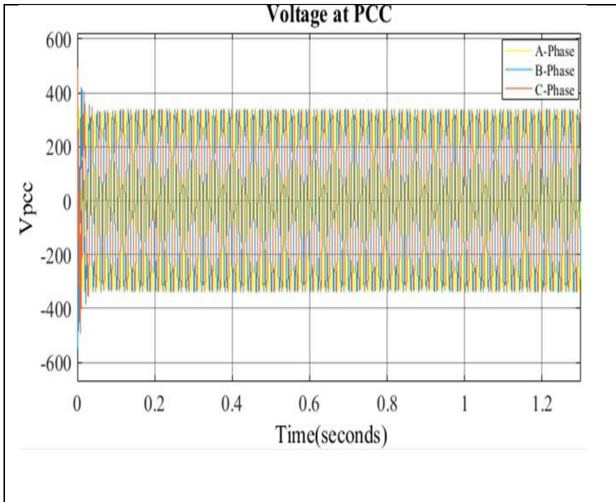

(a)

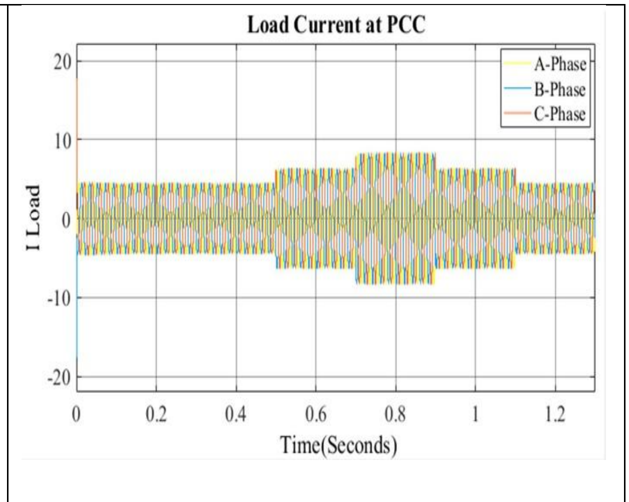

(b)

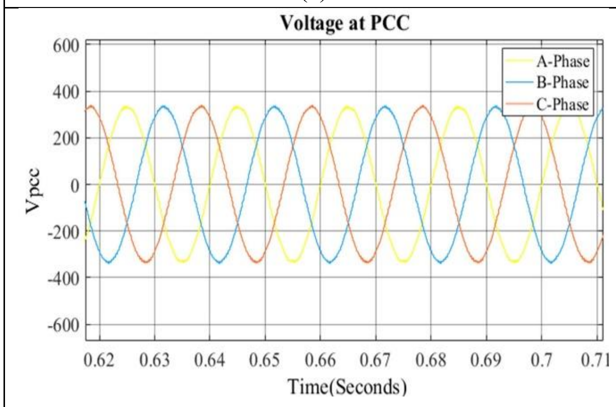

(c)

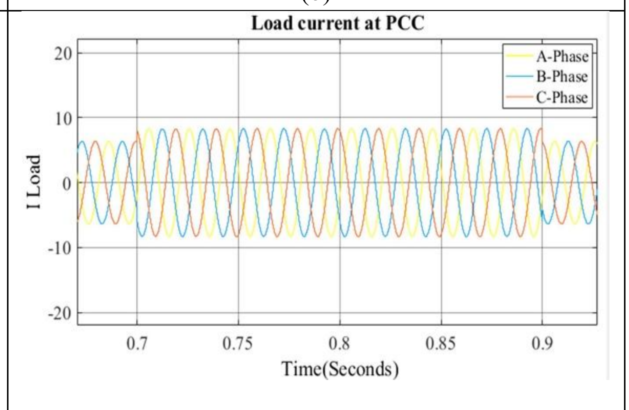

(d)

Fig. 10. PCC voltage and load-current characteristics: (a) PCC voltage waveform, (b) load-current waveform, (c) enlarged view of the PCC voltage, and (d) enlarged view of the load current.

The PCC voltage and load current waveforms, along with their enlarged views, are presented in Fig. 10(a), Fig. 10(b), Fig. 10(c), and Fig. 10(d) for the proposed adaptive neuro fuzzy inference system based control scheme under varying load conditions. The responses maintain sinusoidal nature and exhibit lower harmonic distortion than those obtained with the fuzzy based controller.

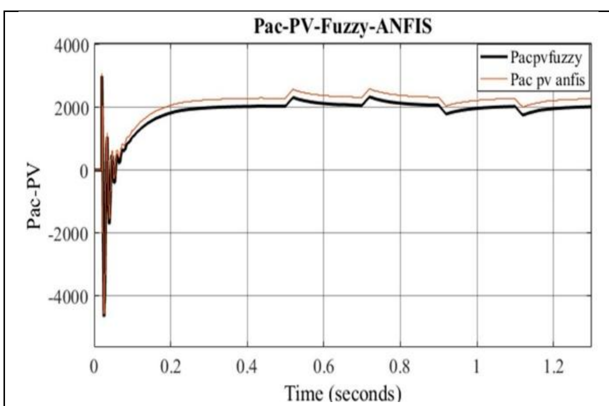

(a)

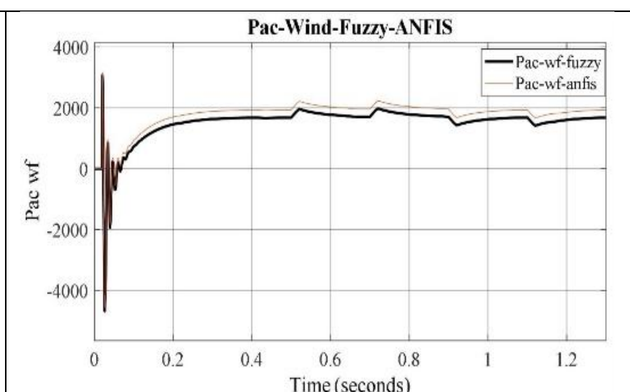

(b)

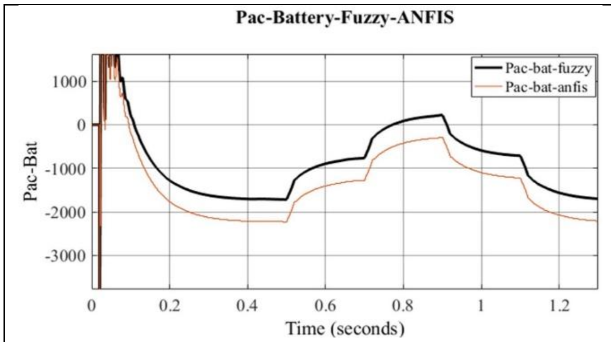

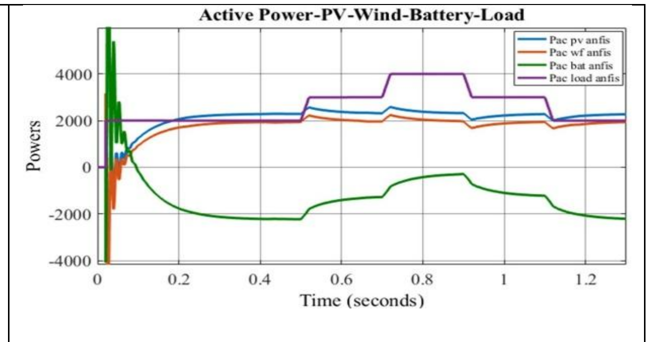

(c) (d)

Fig. 11. Active power characteristics under Fuzzy Logic and ANFIS control: (a) PV array, (b) wind turbine, and (c) battery (d) active power profiles of the PV array, wind turbine, battery, and load.

The active power responses of the PV, wind, and battery subsystems under both FLC and ANFIS control are presented in Fig. 11(a), Fig. 11(b) and Fig. 11 (c) The corresponding power delivered to the AC load is also illustrated, showing the power contribution of each distributed energy source to the overall load demand in Fig. 11 (d).

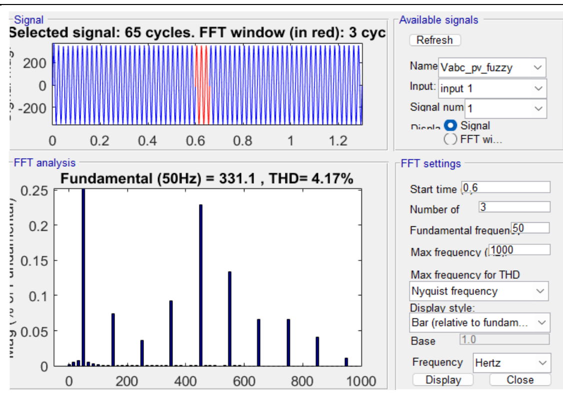

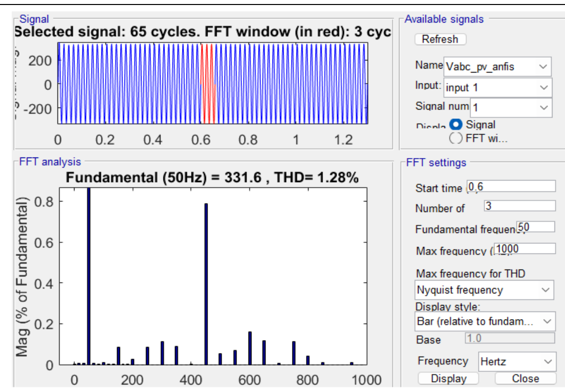

Fig. 12. THD of the PV inverter voltage for FLC and ANFIS assisted control schemes

In Fig.12, the voltage waveform produced by the PV inverter is evaluated using FLC and ANFIS controllers. With FLC, the measured voltage distortion is 4.17% THD, while the ANFIS based controller achieves a lower value of 1.28%. This reduction in harmonic content demonstrates the enhanced voltage waveform quality obtained with the ANFIS control scheme.

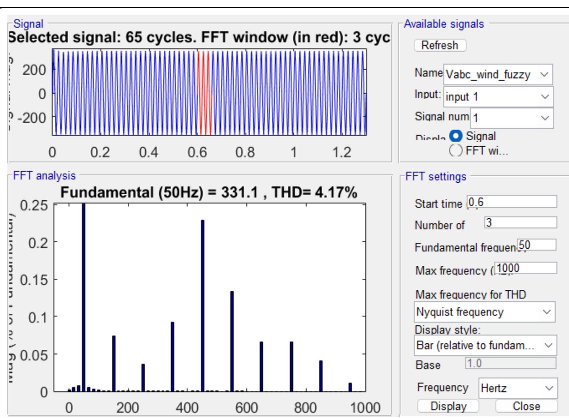

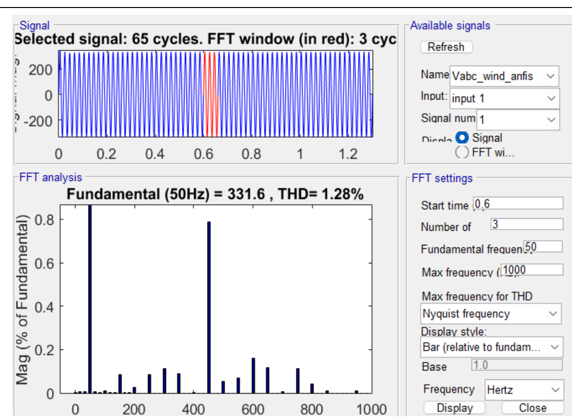

Fig.13. THD of the wind turbine inverter voltage using FLC and ANFIS control techniques.

Fig.13, presents the THD comparison of the wind-turbine inverter output voltage under FLC- and ANFIS-based control. With the FLC, the measured voltage THD is 4.17%. In contrast, the developed ANFIS based scheme limits the voltage distortion to 1.28%, indicating improved waveform quality at the inverter output.

V. CONCLUSION

The developed Adaptive Neuro Fuzzy Inference System provides coordinated energy management for the islanded hybrid renewable energy microgrid under varying generation and load operating conditions. The BESS compensates for the imbalance between renewable generation and load demand, thereby supporting stable power supply and reliable microgrid operation. The developed control strategy coordinates the PV array, wind turbine, and BESS to improve power sharing, renewable energy utilization, and harmonic performance. The developed control framework demonstrates effective energy management and harmonic mitigation in the islanded microgrid system. The developed control strategy reduces THD of PV inverter from 4.1% to 1.28% and THD of wind turbine inverter output voltage from 4.1% to 1.28% . Future work focus on hardware implementation and further improvement of energy management and controller performance under different operating conditions.

REFERENCE

[1] Shahgholian, Ghazanfar. "A brief review on microgrids: Operation, applications, modelling, and control." International Transactions on Electrical Energy Systems 31, no. 6 (2021): e12885.

[2] Punitha, S., N. P. Subramaniam, and P. Ajay D. Vimal Raj. "A comprehensive review of microgrid challenges in architectures, mitigation approaches, and future directions." Journal of Electrical Systems and Information Technology 11, no. 1 (2024): 60.

[3] Abbasi, Maysam, Ehsan Abbasi, Li Li, Ricardo P. Aguilera, Dylan Lu, and Fei Wang. "Review on the microgrid concept, structures, components, communication systems, and control methods." Energies 16, no. 1 (2023): 484.

[4] Fani, Bahador, Ghazanfar Shahgholian, Hassan Haes Alhelou, and Pierluigi Siano. "Inverter-based islanded microgrid: A review on technologies and control." E-prime-advances in electrical engineering, electronics and energy 2 (2022): 100068.

[5] Anderson, Alexander A., and Siddharth Suryanarayanan. "Review of energy management and planning of islanded microgrids." CSEE Journal of Power and Energy Systems 6, no. 2 (2019): 329-343.

[6] Ahmed, Ijaz, Muhammad Rehan, Abdul Basit, Hasnain Ahmad, Waqas Ahmed, Nasim Ullah, Marian Piecha, Vojtech Blazek, and Lukas Prokop. "Review on microgrids design and monitoring approaches for sustainable green energy networks." Scientific Reports 13, no. 1 (2023): 21663.

[7] Shivani, S., P. Rajendar, Dasari Sangeetha, Harshit Goud Naguluri, and Kalagotla Chenchireddy. "Efficiency Enhancement of Solar PV System Through MPPT and Boost Converter Design." In 2025 International Conference on Sustainable Communication Networks and Application (ICSCN), pp. 331-336. IEEE, 2025.

[8] Kumar, Raj, and S. K. Singh. "Solar photovoltaic modeling and simulation: As a renewable energy solution." Energy Reports 4 (2018): 701-712.

[9] Jenisha, C. Maria, N. Ammasai Gounden, and Anmol Agarwal. "Integration of PV array to three-phase grid using Power Electronic converters with de-coupled control." In 2018 20th National Power Systems Conference (NPSC), pp. 1-6. IEEE, 2018.

[10] Diouri, Omar, Najia Es-Sbai, Fatima Errahimi, Ahmed Gaga, and Chakib Alaoui. "Modeling and design of single-phase PV inverter with MPPT algorithm applied to the boost converter using back-stepping control in standalone mode." International Journal of Photoenergy 2019, no. 1 (2019): 7021578.

[11] Sneha, Tabitha, P. S. Kulkarni, Aaditya Rudra, and Soumya Deep Ghosh. "Design and Simulation of a Stand-Alone Hybrid Solar Photovoltaic-Fuel Cell-Battery System in MATLAB Simulink." In 2024 IEEE International Conference on Smart Power Control and Renewable Energy (ICSPCRE), pp. 1-6. IEEE, 2024.

[12] Zou, Ming, Yan Wang, Chengyong Zhao, Jianzhong Xu, Xiaojiang Guo, and Xu Sun. "Integrated equivalent model of permanent magnet synchronous generator based wind turbine for large-scale offshore wind farm simulation." Journal of Modern Power Systems and Clean Energy 11, no. 5 (2023): 1415-1426.

[13] Beik, Omid, and Ahmad Al-Adsani. "Wind turbine productivity and wind energy assessment: An Ontario case study." In 2020 IEEE Electric Power and Energy Conference (EPEC), pp. 1-5. IEEE, 2020.

[14] Moncecchi, Matteo, Claudio Brivio, Stefano Mandelli, and Marco Merlo. "Battery energy storage systems in microgrids: Modeling and design criteria." Energies 13, no. 8 (2020): 2006.

[15] Szilagyi, E., D. Petreus, and T. Patarau. "Optimal energy management for an islanded microgrid with battery degradation cost considerations." In 2024 IEEE 30th International Symposium for Design and Technology in Electronic Packaging (SIITME), pp. 1-6. IEEE, 2024.

[16] Sreelekshmi, R. S., Rishika Lakshmi, and Manjula G. Nair. "AC microgrid with battery energy storage management under grid connected and islanded modes of operation." Energy Reports 8 (2022): 350-357.

[17] Pham, Xuan Hoa Thi. "Power sharing strategy in islanded microgrids using improved droop control." Electric Power Systems Research 180 (2020): 106164.

[18] Sun, Qian, Qiuye Sun, and Dehao Qin. "Adaptive fuzzy droop control for optimized power sharing in an islanded microgrid." Energies 12, no. 1 (2018): 45.

[19] Kim, Sunghyok, Songchol Hyon, and Yongil An. "Harmonic power sharing control using adaptive virtual harmonic impedance in islanded Microgrids." International Journal of Emerging Electric Power Systems 25, no. 2 (2024): 135-148, degruyterbrill.com.

[20] Goh, Hui Hwang, Xiaofeng Zhang, Dongdong Zhang, Wei Dai, Jiefeng Liu, Gaoxiang Li, Tonni Agustiono Kurniawan, and Kai Chen Goh. "Harmonic virtual impedance control in islanded Microgrids for harmonic power sharing and harmonic suppression." CSEE Journal of Power and Energy Systems (2024), ieeexplore.ieee.org.

[21] Budahab, Wajdi, Mahmoud Hamouda, and Kamal Al-Haddad. "A fuzzy logic based controller of DC-link voltage regulation of parallel inverters operation during unintended islanding mode." In IECON 2017-43rd Annual Conference of the IEEE Industrial Electronics Society, pp. 7891-7896. IEEE, 2017.

[22] Kumari, Sushmita, H. M. Suryawanshi, D. Govind, P. P. Nachankar, and Chintalpudi L. Narayana. "A fuzzy logic based load shedding approach for islanding mode of microgrid." In 2021 IEEE international power and renewable energy conference (IPRECON), pp. 1-6. IEEE, 2021.

[23] Bhattacharya, Anagha, Debashis Chatterjee, and Swapan Kumar Goswami. "A fuzzy based improved power sharing methodology for islanded microgrid with hybrid sources." Electric Power Systems Research 217 (2023): 109069.

[24] Pinthurat, Watcharakorn, and Branislav Hredzak. "Fully decentralized control strategy for heterogeneous energy storage systems distributed in islanded DC datacentre microgrid." Energy 231 (2021): 120914.

[25] Rana, Nischay, and Alka Singh. "Control and Modelling of PMSG-Based Wind Turbine for Integration to Conventional Grid." In 2025 IEEE North-East India International Energy Conversion Conference and Exhibition (NE-IECCE), pp. 1-6. IEEE, 2025.

[26] Kulkarni, Haripriya, Amruta Kulkarni, Tejas Pagire, and Sadique Magdum. "Mathematical Modelling, Installation of Wind turbine and its analysis in MATLAB." In 2022 International conference on Electronics and renewable Systems (ICEARS), pp. 142-149. IEEE, 2022.

[27] Jang, J-SR. "ANFIS: adaptive-network-based fuzzy inference system." IEEE transactions on systems, man, and cybernetics 23, no. 3 (1993): 665-685.

[28] Yadaiah, Narri, and Nagireddy Ravi. "Development of Dissolved Gas Analysis Using ANFIS." International Journal on Recent Trends in Engineering & Technology 11, no. 1 (2014): 120.